

Circularly Polarized Gamma Rays in Effective Dark Matter Theory

Wei-Chih Huang¹, Kin-Wang Ng^{2,3} and Tzu-Chiang Yuan²

¹*CP³-Origins, University of Southern Denmark,
Campusvej 55, DK-5230 Odense M, Denmark*

²*Institute of Physics, Academia Sinica, Nangang, Taipei 11529, Taiwan*

³*Institute of Astronomy and Astrophysics,
Academia Sinica, Nangang, Taipei 11529, Taiwan*

(Dated: October 21, 2021)

Abstract

We study the loop-induced circularly polarized gamma rays from dark matter annihilation using the effective dark matter theory approach. Both neutral scalar and fermionic dark matter annihilating into monochromatic diphoton and Z -photon final states are considered. To generate the circular polarization asymmetry, P and CP symmetries must be violated in the couplings between dark matter and Standard Model fermions inside the loop with non-vanishing Cutkosky cut. The asymmetry can be sizable especially for Z -photon final state for which asymmetry of nearly 90% can be reached. We discuss the prospect for detecting the circular polarization asymmetry of the gamma-ray flux from dark matter annihilation in the Galactic Center in future gamma-ray polarimetry experiments.

I. INTRODUCTION

Recent cosmological observations such as the cosmic microwave background, large scale structures, and galactic rotational curves concordantly imply the existence of a large amount of cold dark matter (CDM) in the Universe [1, 2]. The most well-motivated candidate for the CDM is a non-Standard Model (SM) particle such as the lightest supersymmetric particle, extra dimension, hidden sector, and Higgs portal dark matter (DM). So far all experimental searches for these particles remain elusive, giving us stringent constraints to their interactions with the SM sector (see Ref. [3] for a recent review).

Unlike the hunting for DM signals as missing energies in colliders or the direct measurement in cryogenic detectors of the recoil energy of target nuclei bombarded by Galactic halo DM particles, the indirect observation of DM particles accumulated in the Solar core or Galactic Center via their decay or annihilation products such as gamma (γ) rays, positrons, antiprotons, and neutrinos, usually suffers from uncontrollable astrophysical environment and background. There are claims from time to time of excess diffuse or Galactic γ rays and excess positron flux in cosmic rays that are above the astrophysical background, but interpreting the data as the DM signal may be wrong without a thorough removal of the astrophysical uncertainties. As such, any distinct feature of the potential DM signal that helps distinguish DM particles from astrophysical sources would be very invaluable. The capability of detecting polarization in future γ -ray observations will provide a new tool to probe the nature of DM [4]. It is certainly important to explore the possibility for a net linear or circular polarization of γ rays coming from DM annihilations or decays. Recent work along this direction can be found in Refs. [5–11]. Most of these studies are based on specific model buildings. In this *Letter*, we will study the circular polarization of γ rays from DM annihilations using the effective DM theory approach. This is a systematic and model independent way of studying the annihilation of neutral DM particles into γ rays that allows us to obtain the conditions for a net circular polarization of the γ rays.

In the following, we start with the effective operators of interest for both scalar and fermion DM in Sec. II. A little digression addressing the convention of photon polarization as well as fermion spinor wavefunction is devoted in Sec. III. We then proceed to compute loop-induced amplitudes of different photon polarizations for the diphoton final state, followed by the $Z\gamma$ channel in Secs. IV and V respectively. The numerical results are presented in

Sec. VI, and the summary and prospects of future observations are discussed in Sec. VIII.

II. EFFECTIVE DARK MATTER INTERACTIONS

For complex scalar DM, we consider the following dimension 5 effective operator

$$\mathcal{L}^S = \frac{(4\pi)^2}{\Lambda} (\chi^* \chi) (\bar{f} (C_f^S + iC_f^P \gamma_5) f) , \quad (1)$$

where C_f^S and C_f^P are real and f refers to a SM charged fermion. Λ is an effective high cutoff scale which we do not need to specify explicitly.

For Dirac DM, we will focus on three dimension 6 effective operators. The first one is

$$\mathcal{L}_1^D = \frac{(4\pi)^2}{\Lambda^2} (\bar{\chi} (C_\chi^S + iC_\chi^P \gamma_5) \chi) (\bar{f} (C_f^S + iC_f^P \gamma_5) f) , \quad (2)$$

with real $C_{f,\chi}^S$ and $C_{f,\chi}^P$. The second one is

$$\mathcal{L}_2^D = \frac{(4\pi)^2}{\Lambda^2} (\bar{\chi} \gamma_\mu (C_\chi^L P_L + C_\chi^R P_R) \chi) (\bar{f} \gamma^\mu (C_f^L P_L + C_f^R P_R) f) . \quad (3)$$

Since the coefficients $C_{\chi,f}^{L,R}$ are necessarily real, there is no complex parameter in \mathcal{L}_2^D , we do not expect it will give rise to net circular polarization. This will be checked by explicit calculations in Secs. IV and V. The last one is

$$\mathcal{L}_3^D = \frac{(4\pi)^2}{\Lambda^2} (\bar{\chi} \sigma_{\mu\nu} (\tilde{C}_\chi^L P_L + \tilde{C}_\chi^R P_R) \chi) (\bar{f} \sigma^{\mu\nu} (\tilde{C}_f^L P_L + \tilde{C}_f^R P_R) f) , \quad (4)$$

with $\tilde{C}_\chi^R = (\tilde{C}_\chi^L)^*$ and $\tilde{C}_f^R = (\tilde{C}_f^L)^*$. Note that we have normalized the effective operators in Eqs. (1)-(4) according to the naive dimensional analysis [12].

Using the self-duality identities

$$\frac{i}{2} \epsilon^{\alpha\beta\mu\nu} \sigma_{\mu\nu} P_{L,R} = \pm \sigma^{\alpha\beta} P_{L,R} , \quad (5)$$

\mathcal{L}_3^D in Eq. (4) can be rewritten as

$$\mathcal{L}_3^D = \frac{(4\pi)^2}{\Lambda^2} \left[\tilde{C}_{\chi f} (\bar{\chi}_R \sigma_{\mu\nu} \chi_L) (\bar{f}_R \sigma^{\mu\nu} f_L) + \tilde{C}_{\chi f}^* (\bar{\chi}_L \sigma_{\mu\nu} \chi_R) (\bar{f}_L \sigma^{\mu\nu} f_R) \right] , \quad (6)$$

with $\tilde{C}_{\chi f} = \tilde{C}_\chi^L \tilde{C}_f^L$ and $\tilde{C}_{\chi f}^* = \tilde{C}_\chi^R \tilde{C}_f^R = (\tilde{C}_\chi^L \tilde{C}_f^L)^*$.

It is straightforward to extend our analysis to the case of real scalar or Majorana DM. For the Majorana case, we note that $\bar{\chi} \gamma_\mu \chi = 0$, $\bar{\chi} \sigma_{\mu\nu} \chi = 0$, $\bar{\chi} \sigma_{\mu\nu} \gamma_5 \chi = 0$. We will not consider these cases any further here.

III. PHOTON POLARIZATION VECTORS AND FERMION SPINORS

In this section, we specify the convention on photon polarization and fermion spinor wavefunction adopted in this work. Following Refs. [8, 13], a photon traveling with 4-momenta $k^\mu = (k_0, 0, 0, k_z)$ has the right-handed (+) and left-handed (-) circular polarization vectors denoted by

$$\epsilon_{\pm}^\mu = \frac{1}{\sqrt{2}} (\mp \epsilon_1^\mu - i \epsilon_2^\mu) , \quad (7)$$

with

$$\epsilon_1^\mu(k) = (0, 1, 0, 0) \quad , \quad \epsilon_2^\mu(k) = \left(0, 0, \frac{k_z}{|k_z|}, 0 \right) . \quad (8)$$

For the Z boson, besides the above two circular polarization vectors, we also need

$$\epsilon_L^\mu(k) = \frac{1}{m_Z} \left(k, 0, 0, \sqrt{k^2 + m_Z^2} \right) , \quad (9)$$

for the longitudinal component of the Z boson with 3-momentum $\mathbf{k} = k\hat{z}$ along the $+\hat{z}$ direction as we will discuss the $Z\gamma$ final state as well.

On the other hand, assuming the Dirac DM pair annihilates at rest, the four-component spinor for a Dirac DM particle χ of spin $s = 1/2$ in the limit of $v_{\text{DM}} \rightarrow 0$ is

$$u^s(|\vec{p}| = 0) = \sqrt{m_\chi} \begin{pmatrix} \xi^s \\ \xi^s \end{pmatrix} , \quad (10)$$

while for antiparticle, one has

$$v^s(|\vec{p}| = 0) = \sqrt{m_\chi} \begin{pmatrix} \xi^{-s} \\ -\xi^{-s} \end{pmatrix} , \quad (11)$$

where ξ^s denotes the two-component spin wavefunction. Explicitly we have $\xi^{1/2} = (1, 0)^T$ and $\xi^{-1/2} = (0, 1)^T$ corresponding to the DM having spin up and spin down along the $+\hat{z}$ direction.

IV. DRESSING FOR MONOCHROMATIC GAMMA RAYS

Dressing the above effective operators by closing the charged fermion f into a loop, we can discuss DM annihilation into monochromatic gamma rays: $\chi^*\chi \rightarrow \gamma\gamma, Z\gamma$ or $\bar{\chi}\chi \rightarrow \gamma\gamma, Z\gamma$.

We will focus on the $\gamma\gamma$ case in this section and present the $Z\gamma$ case in the next section. In this work, we use `FeynCalc` [14, 15] for analytical computation of one-loop diagrams and `LoopTools` [16] for numerical loop integrals.

We note that the following analysis is based on the effective operators in Eqs. (2), (3), and (4), which involve only fermion final states. As a result, we only consider contributions to $\gamma\gamma$ and $Z\gamma$ states from a specific loop structure, *i.e.*, the triangle diagram in Fig. 1, which includes SM and/or new fermions only. For any UV complete theories such as supersymmetry or hidden sectors, there should exist more loop contributions than triangle diagrams. Those are, however, model-dependent and will not be discussed. Furthermore, our results will not apply to cases where the effective approach breaks down, for example, in the case where the mediator between the DM and SM sectors has a mass much lighter than DM.

To illustrate the applicability of the effective theory approach, in Appendix A we present an exemplary UV vector portal model which can realize \mathcal{L}_2^D in Eq. (3) and will give rise to same results of $\gamma\gamma$ and $Z\gamma$ as derived by our approach. For \mathcal{L}^S and \mathcal{L}_1^D , they can be realized by Higgs portal models, while \mathcal{L}_3^D may be realized by antisymmetric tensor portal models. We will not go into details for these latter models here.

A. Complex Scalar Dark Matter

For complex scalar DM annihilating into two photons via the interaction of \mathcal{L}^S , the calculation is virtually identical to the case of decaying DM studied by Elagin *et al* [9]. In the following, we will adopt the symbols B_0 and C_0 defined in the Passarino-Veltman integrals [17],

$$\begin{aligned} B_0(r_{10}^2, m_0^2, m_1^2) &= \frac{(2\pi\mu)^\epsilon}{i\pi^2} \int d^d k \prod_{i=0}^1 \frac{1}{(k+r_i)^2 - m_i^2}, \\ C_0(r_{10}^2, r_{12}^2, r_{20}^2, m_0^2, m_1^2, m_2^2) &= \frac{(2\pi\mu)^\epsilon}{i\pi^2} \int d^d k \prod_{i=0}^2 \frac{1}{(k+r_i)^2 - m_i^2}, \end{aligned} \quad (12)$$

with the convention of Ref. [14], where $\epsilon = 4 - d$ and $r_{ij}^2 = (r_i - r_j)^2$. In this convention, one has

$$\begin{aligned} (d-4) B_0(4m_\chi^2, m_f^2, m_f^2) &= -2 + \mathcal{O}(\epsilon), \\ C_0(4m_\chi^2, 0, 0, m_f^2, m_f^2, m_f^2) &= -\frac{1}{2m_\chi^2} f(x_f), \end{aligned} \quad (13)$$

where $x_f = m_f^2/m_\chi^2$ and

$$f(x) = \begin{cases} \left(\arcsin \frac{1}{\sqrt{x}} \right)^2 & , \text{ for } x > 1 ; \\ -\frac{1}{4} \left[\log \frac{1 + \sqrt{1-x}}{1 - \sqrt{1-x}} - i\pi \right]^2 & , \text{ for } x \leq 1 . \end{cases} \quad (14)$$

For each internal fermion species, there are two contributions: one shown in the left panel of Fig. 1 plus the other one with the two photons being swapped, $(p_3, \mu) \leftrightarrow (p_4, \nu)$. The amplitude reads

$$\begin{aligned} \mathcal{M}_f &= \mathcal{M}_f^{\mu\nu} \epsilon_\mu^*(p_3) \epsilon_\nu^*(p_4) , \\ \mathcal{M}_f^{\mu\nu} &= -\frac{(4\pi)^2}{\Lambda} i^3 (-ieQ_f)^2 N_C \\ &\quad \times \int \frac{d^d k}{(2\pi)^d} \text{Tr} \left((C_f^S + iC_f^P \gamma_5) \frac{\not{k} - \not{p}_4 + m_f}{(k - p_4)^2 - m_f^2} \gamma^\nu \frac{\not{k} + m_f}{k^2 - m_f^2} \gamma^\mu \frac{\not{k} + \not{p}_3 + m_f}{(k + p_3)^2 - m_f^2} \right. \\ &\quad \left. + (p_3, \mu) \leftrightarrow (p_4, \nu) \right) \\ &= -\frac{m_f}{4\pi^2 m_\chi^2} (eQ_f)^2 N_C \left(\eta_1^{\mu\nu} + 2C_0(4m_\chi^2, 0, 0, m_f^2, m_f^2, m_f^2) \eta_2^{\mu\nu} \right) , \end{aligned} \quad (15)$$

with Q_f and N_C being the electric charge and number of color of f , and

$$\begin{aligned} \eta_1^{\mu\nu} &= C_f^S \left(-2m_\chi^2 g^{\mu\nu} + (1 + 2\Delta B_0) p_3^\mu p_4^\nu + p_3^\nu p_4^\mu \right) , \\ \eta_2^{\mu\nu} &= C_f^P m_\chi^2 \epsilon^{\mu\nu p_3 p_4} + C_f^S \left((m_\chi^2 - m_f^2) (2m_\chi^2 g^{\mu\nu} - p_3^\nu p_4^\mu) + (m_\chi^2 + m_f^2) p_3^\mu p_4^\nu \right) , \end{aligned} \quad (16)$$

where

$$\epsilon^{\mu\nu p_3 p_4} \equiv \epsilon^{\mu\nu\alpha\beta} p_{3\alpha} p_{4\beta} \quad , \quad \Delta B_0 \equiv B_0(4m_\chi^2, m_f^2, m_f^2) - B_0(0, m_f^2, m_f^2) . \quad (17)$$

The polarization transversality makes vanishing contributions from the terms of $p_3^\mu p_4^\nu$ and $p_4^\mu p_3^\nu$.

Based on the definition of the photon polarization vectors in Eqs. (7) and (8), to leading order in v_{DM} , the helicity amplitudes for the two photons in the final state are

$$\mathcal{M}_f(\pm, \mp) = 0 , \quad (18)$$

$$\mathcal{M}_f(+, +) = \frac{(4\pi)^2}{\Lambda} I_f(+, +) , \quad \mathcal{M}_f(-, -) = \frac{(4\pi)^2}{\Lambda} I_f(-, -) , \quad (19)$$

with

$$\mathcal{I}_f(+, +) = \frac{2N_C Q_f^2 \alpha_{\text{em}}}{\pi} m_f \left[((x_f - 1) f(x_f) - 1) C_f^S + i f(x_f) C_f^P \right] , \quad (20)$$

$$\mathcal{I}_f(-, -) = \frac{2N_C Q_f^2 \alpha_{\text{em}}}{\pi} m_f \left[((x_f - 1) f(x_f) - 1) C_f^S - i f(x_f) C_f^P \right] , \quad (21)$$

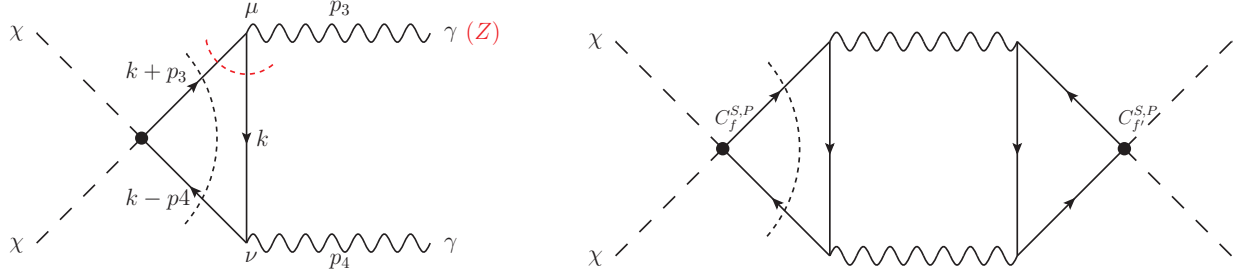


FIG. 1. Left: A representative loop diagram for DM annihilates into two photons, where curly dashed lines indicate Cutkosky cuts on internal fermions which are required for polarization asymmetry. See the main text for details. Right: Illustration of dominant contributions from the interference of heavy-light fermions to polarization asymmetry.

where $\alpha_{\text{em}} = e^2/(4\pi)$, $x_f = m_f^2/m_\chi^2$ and $f(x)$ is defined in Eq. (14). The result is in agreement with Ref. [9]. If $x_f > 1$, then $f(x_f)$ is real. This implies $\mathcal{I}_f(-, -) = (\mathcal{I}_f(+, +))^*$, and thus there will be no net circular polarization even though CP is violated by complex couplings. On the other hand, if $x_f \leq 1$, then $f(x_f)$ is complex and in general $|\mathcal{I}_f(+, +)|^2 \neq |\mathcal{I}_f(-, -)|^2$. It corresponds to the internal fermions being on-shell marked by the black dashed line (Cutkosky cut) in the left panel of Fig. 1. As a result, a net circular polarization can be produced in this case. Note that there are in fact three possibilities of having complex loop integrals which are correlated with Cutkosky cuts on any two of the three internal fermions. As we shall see below, when one of the outgoing photons is replaced by the massive Z boson, there exists more nontrivial region of the parameter space that can induce polarization symmetry, as indicated by the red dashed Cutkosky cut on the internal fermions connected to Z .

In reality, we need to sum over all possible charged fermions running inside the loop.

$$|\mathcal{M}|^2 = \left| \sum_f \mathcal{M}_f(+, +) \right|^2 + \left| \sum_f \mathcal{M}_f(-, -) \right|^2. \quad (22)$$

Therefore, there are mixing terms between contributions from different fermions leading to complicated expressions of the asymmetry between the $(+, +)$ and $(-, -)$ polarizations. Although directly from Eqs. (20) and (21) it is straightforward to infer the total asymmetry including all contributions, for illustrative purposes we show only the asymmetry due to a

single fermion field f in the loop:

$$\left(\left| \mathcal{M}_f(+, +) \right|^2 - \left| \mathcal{M}_f(-, -) \right|^2 \right) = 8 \left(\frac{N_C Q_f^2 \alpha_{\text{em}}}{\pi} m_f \right)^2 C_f^2 |f(x_f)| \sin 2\theta_1 \sin \theta_2, \quad (23)$$

where

$$C_f = \sqrt{C_f^{S^2} + C_f^{P^2}}, \quad C_f^P = C_f \sin \theta_1 \quad \text{and} \quad f(x_f) = |f(x_f)| (\cos \theta_2 + i \sin \theta_2). \quad (24)$$

It is clear that the asymmetry requires two complex phases associated with the coupling constants and the loop integrals, respectively. In addition, both C_f^S and C_f^P have to be nonzero; otherwise, one can always rotate away the phase θ_1 by field redefinition.

Due to the fact that the amplitude is proportional to m_f , in case DM is heavier than all of possible internal fermions and the effective couplings are roughly the same order for the fermions, dominant contributions to polarization asymmetry will come from the heaviest fermions. On the other hand, when the DM mass is among the fermion ones, the main contributions arise from the heavy-light interference where the heavy internal fermion provides a complex coupling constant while the light-fermion loop supplies a complex loop integral as demonstrated in the right panel of Fig. 1.

B. Dirac Dark Matter

Here we consider effective operators $\mathcal{L}_{1,2,3}^D$ for Dirac DM. Consider $\chi(k_1, s_1) \bar{\chi}(k_2, s_2) \rightarrow \gamma(k_3, h_3) \gamma(k_4, h_4)$, where (k_1, s_1) and (k_2, s_2) are the momenta/helicities of the DM χ and $\bar{\chi}$, and (k_3, h_3) and (k_4, h_4) are the momenta/helicities of the two final state photons. Denote the helicity amplitude for the process as $\mathcal{M}(s_1, s_2; h_3, h_4)$. Summing over the initial spins of the DM, we have

$$|\mathcal{M}(h_3, h_4)|^2 = \sum_{s_1, s_2} |\mathcal{M}(s_1, s_2; h_3, h_4)|^2. \quad (25)$$

1. \mathcal{L}_1^D

The calculation for this case is very similar to \mathcal{L}^S .

$$|\mathcal{M}(h_3, h_4)|^2 = \frac{(4\pi)^4}{\Lambda^4} \left[(k_1 \cdot k_2 - m_\chi^2) (C_\chi^S)^2 + (k_1 \cdot k_2 + m_\chi^2) (C_\chi^P)^2 \right] \left| \sum_f \mathcal{I}_f(h_3, h_4) \right|^2. \quad (26)$$

$\mathcal{I}_f(h_3, h_4)$ is the helicity amplitude of the two photon final state. Again to leading order in v_{DM} , the only non-vanishing components are $\mathcal{I}_f(+, +)$ and $\mathcal{I}_f(-, -)$ given by (20) and (21) respectively. For non-relativistic DM, $k_1 = k_2 \approx (m_\chi, \vec{0})$ and $k_1 \cdot k_2 = m_\chi^2$. We then have the simpler result

$$|\mathcal{M}(h_3, h_4)|^2 \approx \frac{(4\pi)^4}{\Lambda^4} 2m_\chi^2 (C_\chi^P)^2 \left| \sum_f \mathcal{I}_f(h_3, h_4) \right|^2. \quad (27)$$

Note that C_χ^S has dropped out in the non-relativistic limit because of velocity suppression. Again since in general we have $|\sum_f \mathcal{I}_f(+, +)|^2 \neq |\sum_f \mathcal{I}_f(-, -)|^2$, net circular polarization will be produced from $\chi\bar{\chi} \rightarrow \gamma\gamma$ via \mathcal{L}_1^D . The circular polarization asymmetry from a single fermion species is proportional to

$$\frac{1}{4} \left(\left| \mathcal{M}_f(+, +) \right|^2 - \left| \mathcal{M}_f(-, -) \right|^2 \right) = 16 \left(\frac{N_C Q_f^2 \alpha_{\text{em}} m_f m_\chi}{\pi} \right)^2 C_\chi^{P^2} C_f^2 |f(x_f)| \sin 2\theta_1 \sin \theta_2, \quad (28)$$

which is identical to Eq. (23) up to a factor of $2m_\chi^2 C_\chi^{P^2}$.

2. \mathcal{L}_2^D

Although it is not expected that \mathcal{L}_2^D will give rise to net circular polarization as all the couplings are real, we however check this statement by explicit calculation. For $\chi(p_1) \bar{\chi}(p_2) \rightarrow \gamma(\epsilon^\mu(p_3)) \gamma(\epsilon^\nu(p_4))$, the DM side has the amplitude

$$\mathcal{M}_\sigma(\text{DM}) = \frac{(4\pi)^2}{\Lambda^2} \sum_{s, s'} \overline{v^{s'}(p_2)} \gamma_\sigma (C_\chi^L P_L + C_\chi^R P_R) u(p_1)^s, \quad (29)$$

while the SM side has

$$\begin{aligned} \mathcal{M}_f^\sigma(\text{SM}) &= \mathcal{M}_f^{\sigma\mu\nu} \epsilon_\mu^*(p_3) \epsilon_\nu^*(p_4), \\ \mathcal{M}_f^{\sigma\mu\nu} &= (-1) i^3 (-ieQ_f)^2 N_C \frac{(C_f^R - C_f^L)}{2} \\ &\quad \times \int \frac{d^d k}{(2\pi)^d} \text{Tr} \left(\gamma^\sigma \gamma^5 \frac{\not{k} - \not{p}_4 + m_f}{(k - p_4)^2 - m_f^2} \gamma^\nu \frac{\not{k} + m_f}{k^2 - m_f^2} \gamma^\mu \frac{\not{k} + \not{p}_3 + m_f}{k^2 - m_f^2} \right. \\ &\quad \left. + (p_3, \mu) \leftrightarrow (p_4, \nu) \right), \\ &= (-i) (eQ_f)^2 N_C \frac{(C_f^R - C_f^L)}{2} \\ &\quad \times [\lambda_1^{\sigma\mu\nu} \Delta B_0 + \lambda_2^{\sigma\mu\nu} (1 + 2m_f^2 C_0 (4m_\chi^2, 0, 0, m_f^2, m_f^2, m_f^2))] , \end{aligned} \quad (30)$$

with

$$\begin{aligned}\lambda_1^{\sigma\mu\nu} &= \frac{1}{8\pi^2 m_\chi^2} (\epsilon^{\sigma\nu p_3 p_4} p_3^\mu - \epsilon^{\sigma\mu p_3 p_4} p_4^\nu) , \\ \lambda_2^{\sigma\mu\nu} &= \frac{1}{8\pi^2 m_\chi^2} (\epsilon^{\sigma\mu p_3 p_4} p_3^\nu - \epsilon^{\sigma\nu p_3 p_4} p_4^\mu + 2m_\chi^2 (\epsilon^{\sigma\mu\nu p_3} - \epsilon^{\sigma\mu\nu p_4})) ,\end{aligned}\quad (31)$$

where $\epsilon^{\sigma\mu\nu p(3,4)} = \epsilon^{\sigma\mu\nu\kappa} p_{(3,4)\kappa}$. Again, the $\lambda_1^{\sigma\mu\nu}$ term will not contribute as transversality of the photon polarization vectors dictates $p_3^\mu \epsilon_\mu(p_3) = p_4^\nu \epsilon_\nu(p_4) = 0$, which is not the case if the photon is replaced by the Z boson that has a longitudinal component. Note that the term proportional $C_f^R + C_f^L$ (γ^σ term) is vanishing due to Furry's theorem from charge conjugation (C) invariance in QED. In addition, our results are consistent with Ref. [18], which demonstrates that the amplitude $\mathcal{M}_f^{\sigma\mu\nu}$ can in general be decomposed into six terms. The corresponding coefficients are correlated as a result of the invariance under the two photon exchange, $(\mu, p_3) \leftrightarrow (\nu, p_4)$, and the Ward-Takahashi identity: $\mathcal{M}_f^{\sigma\mu\nu} p_{3\mu} = \mathcal{M}_f^{\sigma\mu\nu} p_{4\nu} = 0$. See, for instance, Stephen L. Adler's lecture on "Perturbation Theory Anomalies" in [19] for a pedagogical review.

Furthermore, one can reproduce computation of the well-known axial current anomaly by contracting the amplitude with the total momentum in the limit of $m_f \rightarrow 0$:

$$i(p_3 + p_4)_\sigma \mathcal{M}_f^\sigma(\text{SM}) = -(eQ_f)^2 N_C \frac{(C_f^R - C_f^L)}{2} \frac{\epsilon^{\epsilon_3^* \epsilon_4^* p_3 p_4}}{2\pi^2}. \quad (32)$$

By combining the DM and SM amplitudes and with the help of Eqs. (7) to (11), one has for the amplitude squared

$$|\overline{\mathcal{M}}|^2 = \frac{1}{4} \left(\left| \sum_f \mathcal{M}_f(+, +) \right|^2 + \left| \sum_f \mathcal{M}_f(-, -) \right|^2 \right), \quad (33)$$

where to leading order in v_{DM} ,

$$\mathcal{M}_f(\pm, \mp) = 0, \quad (34)$$

$$\mathcal{M}_f(\pm, \pm) = \frac{(4\pi)^2 \sqrt{2} N_C Q_f^2 \alpha_{\text{em}} m_\chi^2}{\Lambda^2 \pi} (C_\chi^R - C_\chi^L) (C_f^R - C_f^L) (1 - x_f f(x_f)). \quad (35)$$

Since $|\sum_f \mathcal{M}_f(+, +)|^2 = |\sum_f \mathcal{M}_f(-, -)|^2$, there is no net circular polarization as expected from general argument of the lack of complex couplings in \mathcal{L}_2^D .

3. \mathcal{L}_3^D

For \mathcal{L}_3^D , the calculation is straightforward but tedious. The DM side has the amplitude

$$\mathcal{M}_{\alpha\beta}(\text{DM}) = \frac{(4\pi)^2}{\Lambda^2} \sum_{s,s'} \overline{v^{s'}(p_2)} \sigma_{\alpha\beta} \left(\tilde{C}_\chi^L P_L + \tilde{C}_\chi^R P_R \right) u(p_1)^s, \quad (36)$$

while the SM side has

$$\begin{aligned} \mathcal{M}_f^{\alpha\beta}(\text{SM}) &= \mathcal{M}_f^{\alpha\beta\mu\nu} \epsilon_\mu^*(p_3) \epsilon_\nu^*(p_4), \\ \mathcal{M}_f^{\alpha\beta\mu\nu} &= (-1) i^3 (-ieQ_f)^2 N_C \frac{(\tilde{C}_f^R - \tilde{C}_f^L)}{2} \\ &\quad \times \int \frac{d^d k}{(2\pi)^d} \text{Tr} \left(\sigma^{\alpha\beta} \gamma^5 \frac{\not{k} - \not{p}_4 + m_f}{(k - p_4)^2 - m_f^2} \gamma^\nu \frac{\not{k} + m_f}{k^2 - m_f^2} \gamma^\mu \frac{\not{k} + \not{p}_3 + m_f}{(k + p_3)^2 - m_f^2} \right. \\ &\quad \left. + (p_3, \mu) \leftrightarrow (p_4, \nu) \right), \\ &= (-i)(eQ_f)^2 N_C \frac{(\tilde{C}_f^R - \tilde{C}_f^L)}{2} \kappa_1^{\alpha\beta\mu\nu} C_0(4m_\chi^2, 0, 0, m_f^2, m_f^2, m_f^2), \end{aligned} \quad (37)$$

with

$$\kappa_1^{\alpha\beta\mu\nu} = \frac{m_f}{4\pi^2} \left(g^{\alpha\mu} \epsilon^{\beta\nu p_3 p_4} - g^{\alpha\nu} \epsilon^{\beta\mu p_3 p_4} + p_3^\alpha \epsilon^{\beta\mu\nu p_4} - p_4^\alpha \epsilon^{\beta\mu\nu p_3} - (\alpha \leftrightarrow \beta) \right). \quad (38)$$

Based on Eqs. (7), (10) and (11), it is straightforward to show that $\kappa_1^{\alpha\beta\mu\nu}$ is zero after contracting with $\epsilon_\mu^*(p_3) \epsilon_\nu^*(p_4)$ and $\sigma_{\alpha\beta}$ on indices α, β, μ and ν .

A simple way to understand the vanishing amplitude is to notice that the initial state corresponding to either the magnetic or electric dipole moment is odd under C , whereas each of the two photons in the final state is also odd under C . It leads to a vanishing amplitude according to the Furry's theorem.

Another way to understand this is to see if one can write down effective operators to describe the amplitude. Due to gauge invariance one needs to involve two EM field strength. Possible effective operators are

$$\bar{\chi} \sigma_{\mu\nu} \left(\tilde{C}_\chi^L P_L + \tilde{C}_\chi^R P_R \right) \chi F^{\mu\alpha} F_\alpha^\nu, \quad (39)$$

$$\bar{\chi} \sigma_{\mu\nu} \left(\tilde{C}_\chi^L P_L + \tilde{C}_\chi^R P_R \right) \chi \epsilon^{\mu\nu\rho\sigma} F_{\rho\alpha} F_\sigma^\alpha, \quad (40)$$

$$\bar{\chi} \sigma_{\mu\nu} \left(\tilde{C}_\chi^L P_L + \tilde{C}_\chi^R P_R \right) \chi F^{\mu\alpha} \tilde{F}_\alpha^\nu. \quad (41)$$

The first two operators vanish identically. The third operator is non-zero, but as demonstrated by explicit calculation above, its coefficient is zero.

V. $Z\gamma$ FINAL STATE

Here we collect the results for the $Z\gamma$ final state, where we sum over three Z polarizations: right-handed (+), left-handed (−) and longitudinal (L) polarizations. Note that for the following results, we have explicitly checked that the Goldstone boson equivalence theorem (for $Z(p_3)$) and the Ward-Takahashi identity (for $\gamma(p_4)$) hold respectively. That is, $\mathcal{M}^{\alpha\cdots\mu\nu}p_{3\mu} = m_Z\mathcal{M}^{\alpha\cdots\nu}$ and $\mathcal{M}^{\alpha\cdots\mu\nu}p_{4\nu} = 0$, where m_Z is the Z mass.

A. Complex Scalar Dark Matter

Due to conservation of angular momentum, only the (+, +) and (−, −) helicity configurations with the first (second) entry refers to the Z (γ) polarization have nonzero amplitudes.

$$|\mathcal{M}|^2 = \left| \sum_f \mathcal{M}_f(+, +) \right|^2 + \left| \sum_f \mathcal{M}_f(-, -) \right|^2, \quad (42)$$

where to leading order in v_{DM} , $\mathcal{M}_f(\pm, \mp) = \mathcal{M}_f(L, \pm) = 0$ and

$$\begin{aligned} \mathcal{M}_f(+, +) &= \frac{2y_s}{\pi} \frac{(4\pi)^2}{\Lambda} \frac{4 - x_Z}{4} m_f \left[-\frac{\rho_1}{(4 - x_Z)^2} C_f^S + i\rho_2 C_f^P \right], \\ \mathcal{M}_f(-, -) &= \frac{2y_s}{\pi} \frac{(4\pi)^2}{\Lambda} \frac{4 - x_Z}{4} m_f \left[-\frac{\rho_1}{(4 - x_Z)^2} C_f^S - i\rho_2 C_f^P \right], \end{aligned} \quad (43)$$

with

$$\begin{aligned} \rho_1 &= 16 + g(x_f, x_Z) (4 - x_Z) (4 - 4x_f - x_Z) + 4x_Z \Delta B_1, \\ \rho_2 &= g(x_f, x_Z), \end{aligned} \quad (44)$$

where $x_Z = m_Z^2/m_\chi^2$, $y_s = N_C Q_f^2 z_V \alpha_{\text{em}}$ (with the vector coupling z_V defined in Eq. (46) below) and

$$\begin{aligned} g(x_f, x_Z) &\equiv -2 m_\chi^2 C_0 (4m_\chi^2, m_Z^2, 0, m_f^2, m_f^2, m_f^2), \\ \Delta B_1 &\equiv B_0 (4m_\chi^2, m_f^2, m_f^2) - B_0 (m_Z^2, m_f^2, m_f^2) - 1. \end{aligned} \quad (45)$$

Note that $g(x_f, x_Z)$ and ΔB_1 can be complex if the internal fermions are on-shell, where complex $B_0 (4m_\chi^2, m_f^2, m_f^2)$ and $B_0 (m_Z^2, m_f^2, m_f^2)$ correspond to two Cutkosky cuts marked by the black and red dashed lines respectively in the left-panel of Fig. 1.

The symbol z_V corresponds to the fermion vector coupling¹ to Z normalized to the corresponding electric charge. For instance, with the internal electron one has

$$z_V = \frac{1}{eQ_e} \frac{g}{\cos \theta_W} \left(\frac{T^3 - 2 \sin^2 \theta_W Q_e}{2} \right), \quad (46)$$

where g is the SM $SU(2)_L$ gauge coupling, e is the electric coupling, θ_W is the Weinberg angle, $Q_e = -1$ and $T^3 = -1/2$. In the following, we will also use the symbol z_A for the axial current, *e.g.*,

$$z_A = \frac{1}{eQ_e} \frac{g}{\cos \theta_W} \left(-\frac{T^3}{2} \right), \quad (47)$$

for the electron. Note that one can reproduce Eqs. (20) and (21) above by setting $x_Z = 0$, $z_V = 1$, and $g(x_f, x_Z) \rightarrow f(x_f)$. The circular polarization asymmetry from contributions of a fermion f is proportional to

$$\begin{aligned} & \left| \mathcal{M}_f(+, +) \right|^2 - \left| \mathcal{M}_f(-, -) \right|^2 \\ &= \frac{(4\pi)^4}{\Lambda^4} \frac{2y_s^2 x_f}{\pi^2} C_f^2 |g(x_f, x_Z)| \sin 2\theta_1 (4 \sin \theta'_2 + x_Z |\Delta B_1| \sin(\theta'_2 - \theta_3)), \end{aligned} \quad (48)$$

where

$$g(x_f, x_Z) = |g(x_f, x_Z)| (\cos \theta'_2 + i \sin \theta'_2) \quad \text{and} \quad \Delta B_1 = |\Delta B_1| (\cos \theta_3 + i \sin \theta_3). \quad (49)$$

B. Dirac Dark Matter

1. \mathcal{L}_1^D

As mentioned above in the diphoton case, at amplitude-squared level the result is similar to that of the scalar DM case, except for an additional factor from the trace of DM spinor wavefunctions. In the limit of zero DM velocity, the asymmetry is simply given by Eq. (48) multiplied by $2m_\chi^2 (C_\chi^P)^2$.

2. \mathcal{L}_2^D

One has for the amplitude squared

¹ The Z axial current does not contribute due to the Furry's theorem as the axial current is even under C .

$$\overline{|\mathcal{M}|^2} = \frac{1}{4} \left(\left| \sum_f \mathcal{M}_f(+, +) \right|^2 + \left| \sum_f \mathcal{M}_f(L, +) \right|^2 + \left| \sum_f \mathcal{M}_f(-, -) \right|^2 + \left| \sum_f \mathcal{M}_f(L, -) \right|^2 \right), \quad (50)$$

where $|\mathcal{M}_f(+, +)|^2 = |\mathcal{M}_f(-, -)|^2$ and $|\mathcal{M}_f(L, +)|^2 = |\mathcal{M}_f(L, -)|^2$. For contributions from a fermion f , we obtain, to leading order in v_{DM} , $\mathcal{M}_f(\pm, \mp) = 0$ and

$$\begin{aligned} |\mathcal{M}_f(+, +)|^2 &= y_V^2 \frac{(4\pi)^4}{\Lambda^4} \frac{1}{8\pi^2} \left(\frac{|\kappa_1^f|^2}{(4-x_Z)^2} (C_\chi^R + C_\chi^L)^2 + |\kappa_2^f|^2 (C_\chi^R - C_\chi^L)^2 \right), \\ |\mathcal{M}_f(L, +)|^2 &= y_V^2 \frac{(4\pi)^4}{\Lambda^4} \frac{1}{2\pi^2} \frac{|\kappa_1^f|^2}{x_Z(4-x_Z)^2} (C_\chi^R + C_\chi^L)^2, \end{aligned} \quad (51)$$

with $y_V = N_C Q_f^2 \alpha_{\text{em}} m_\chi^2$. The coefficients κ_1^f and κ_2^f are

$$\begin{aligned} \kappa_1^f &= (C_f^R + C_f^L) z_A (-4g(x_f, x_Z) x_f (4-x_Z) + x_Z (8-x_Z + 4\Delta B_1)) \\ &\quad + (C_f^R - C_f^L) x_Z z_V (8-g(x_f, x_Z) x_f (4-x_Z) - x_Z + 4\Delta B_1), \\ \kappa_2^f &= (4-x_Z) ((C_f^R + C_f^L) z_A + (C_f^R - C_f^L) z_V (1-g(x_f, x_Z) x_f)). \end{aligned} \quad (52)$$

It is straightforward to generalize to cases with more than one fermion by the replacement

$$Q_f^2 \kappa_i^f \rightarrow \sum_f Q_f^2 \kappa_i^f,$$

for $i = (1, 2, 3)$. Note again that by setting $z_A = 0$, $x_Z = 0$ ($m_Z = 0$) and $z_V = 1$ which implies $\kappa_1^f = 0$ and hence the longitudinal component drops, Eq. (34) is reproduced. Due to Furry's theorem, the contribution from the SM fermion vector current (axial current) is nonzero only in the presence of the the Z axial current (vector current). Nevertheless just like the diphoton case there is no asymmetry in this Z -photon case as well due to the lack of complex couplings for CP violation in \mathcal{L}_2^D .

3. \mathcal{L}_3^D

Similarly, one has for the amplitude squared

$$\overline{|\mathcal{M}|^2} = \frac{1}{4} \left(\left| \sum_f \mathcal{M}_f(+, +) \right|^2 + \left| \sum_f \mathcal{M}_f(L, +) \right|^2 + \left| \sum_f \mathcal{M}_f(-, -) \right|^2 + \left| \sum_f \mathcal{M}_f(L, -) \right|^2 \right). \quad (53)$$

For contributions from a fermion f , one has to leading order in v_{DM} ,

$$\begin{aligned}
|\mathcal{M}_f(+, +)|^2 &= y_A^2 \frac{(4\pi)^4}{\Lambda^4} \frac{16 x_f}{(4 - x_Z)^2 \pi^2} \left| \sqrt{2} \tilde{C}_{\chi f}^* \lambda_1 + \frac{1}{\sqrt{2}} \tilde{C}_{\chi f} \lambda_2 \right|^2 \\
&= y_A^2 \frac{(4\pi)^4}{\Lambda^4} \frac{16 x_f}{(4 - x_Z)^2 \pi^2} \left(\left(\tilde{C}_{\chi f}^2 \lambda_1^* \lambda_2 + \tilde{C}_{\chi f}^{r*2} \lambda_1 \lambda_2^* \right) + \frac{\tilde{C}_{\chi f} \tilde{C}_{\chi f}^*}{2} (4|\lambda_1|^2 + |\lambda_2|^2) \right), \\
|\mathcal{M}_f(-, -)|^2 &= y_A^2 \frac{(4\pi)^4}{\Lambda^4} \frac{16 x_f}{(4 - x_Z)^2 \pi^2} \left| \sqrt{2} \tilde{C}_{\chi f} \lambda_1 + \frac{1}{\sqrt{2}} \tilde{C}_{\chi f}^* \lambda_2 \right|^2 \\
&= y_A^2 \frac{(4\pi)^4}{\Lambda^4} \frac{16 x_f}{(4 - x_Z)^2 \pi^2} \left(\left(\tilde{C}_{\chi f}^2 \lambda_1 \lambda_2^* + \tilde{C}_{\chi f}^{r*2} \lambda_1^* \lambda_2 \right) + \frac{\tilde{C}_{\chi f} \tilde{C}_{\chi f}^*}{2} (4|\lambda_1|^2 + |\lambda_2|^2) \right), \\
|\mathcal{M}_f(L, +)|^2 &= y_A^2 \frac{(4\pi)^4}{\Lambda^4} \frac{32 x_f}{(4 - x_Z)^2 \pi^2} \left| 2 \tilde{C}_{\chi f}^* \lambda_1 + \frac{1}{2} \tilde{C}_{\chi f} \lambda_3 \right|^2 \\
&= y_A^2 \frac{(4\pi)^4}{\Lambda^4} \frac{32 x_f}{(4 - x_Z)^2 \pi^2} \left(\left(\tilde{C}_{\chi f}^2 \lambda_1^* \lambda_3 + \tilde{C}_{\chi f}^{r*2} \lambda_1 \lambda_3^* \right) + \frac{\tilde{C}_{\chi f} \tilde{C}_{\chi f}^*}{4} (16|\lambda_1|^2 + |\lambda_3|^2) \right), \\
|\mathcal{M}_f(L, -)|^2 &= y_A^2 \frac{(4\pi)^4}{\Lambda^4} \frac{32 x_f}{(4 - x_Z)^2 \pi^2} \left| 2 \tilde{C}_{\chi f} \lambda_1 + \frac{1}{2} \tilde{C}_{\chi f}^* \lambda_3 \right|^2 \\
&= y_A^2 \frac{(4\pi)^4}{\Lambda^4} \frac{32 x_f}{(4 - x_Z)^2 \pi^2} \left(\left(\tilde{C}_{\chi f}^2 \lambda_1 \lambda_3^* + \tilde{C}_{\chi f}^{r*2} \lambda_1^* \lambda_3 \right) + \frac{\tilde{C}_{\chi f} \tilde{C}_{\chi f}^*}{4} (16|\lambda_1|^2 + |\lambda_3|^2) \right), \\
\mathcal{M}_f(\pm, \mp) &= 0,
\end{aligned} \tag{54}$$

with $y_A = N_C z_A Q_f^2 \alpha_{\text{em}} m_\chi^2$ and

$$\begin{aligned}
\lambda_1 &= 4 - x_f g(x_f, x_Z) (4 - x_Z) + x_Z \Delta B_1, \\
\lambda_2 &= g(x_f, x_Z) (4 - x_Z) (-4 - 2x_f + x_Z) - 2x_Z (2 + \Delta B_1) + 8(3 + 2\Delta B_1),
\end{aligned} \tag{55}$$

$$\begin{aligned}
\lambda_3 &= -16(1 + \Delta B_0 + \Delta B_1) \\
&\quad + x_Z [12 - x_f g(x_f, x_Z) (4 - x_Z) + 8\Delta B_0 - x_Z (1 + \Delta B_0) + 8\Delta B_1].
\end{aligned} \tag{56}$$

Similarly, it is straightforward to generalize to cases of multiple fermions by factoring in z_A and m_f (terms depending on fermion properties) and summing up contributions within $|\cdot|^2$, *i.e.*, $|\text{Stuff}_f|^2 \rightarrow |\sum_f \text{Stuff}_f|^2$. It is clear by setting $z_A = 0$, the amplitude vanishes as in the two photon final state. However, with the $Z\gamma$ final state, the polarization asymmetry can be generated if \tilde{C} s are complex and the internal particles are on-shell.

For illustration, the circular polarization asymmetry resulting from a single fermion con-

tribution is proportional to

$$\begin{aligned} & \frac{1}{4} \left(\left| \mathcal{M}_f(+, +) \right|^2 + \left| \mathcal{M}_f(L, +) \right|^2 - \left| \mathcal{M}_f(-, -) \right|^2 - \left| \mathcal{M}_f(L, -) \right|^2 \right) \\ & = \frac{(4\pi)^4}{\Lambda^4} \frac{16 y_A^2 x_f}{\pi^2 x_Z} |\tilde{C}_{\chi f}|^2 \sin(2\theta_{\chi f}) (2t_1 + t_2 + 2t_3) , \end{aligned} \quad (57)$$

where

$$\begin{aligned} \tilde{C}_{\chi f} & = |\tilde{C}_{\chi f}| (\cos \theta_{\chi f} + i \sin \theta_{\chi f}) , \\ t_1 & = |g(x_f, x_Z)| \sin \theta'_2 (2x_Z + x_f (4 - 3x_Z)) , \\ t_2 & = |g(x_f, x_Z)| |\Delta B_1| \sin(\theta'_2 - \theta_3) (x_Z^2 + x_f (8 - 6x_Z)) , \\ t_3 & = |\Delta B_1| \sin \theta_3 (4 - 3x_Z) + |\Delta B_0| \left(x_f |g(x_f, x_Z)| \sin(\theta'_2 - \theta_4) (4 - x_Z) \right. \\ & \quad \left. - x_Z |\Delta B_1| \sin(\theta_3 - \theta_4) + 4 \sin \theta_4 \right) , \end{aligned} \quad (58)$$

and $\Delta B_0 = |\Delta B_0| (\cos \theta_4 + i \sin \theta_4)$.

Here we summarize our theoretical calculation. In the diphoton final state, only two effective operators \mathcal{L}^S and \mathcal{L}_1^D can give rise to circular polarization asymmetry, whereas in the Z -photon final state, besides \mathcal{L}^S and \mathcal{L}_1^D , \mathcal{L}_3^D can also generate the asymmetry. It is necessary in each non-vanishing case to have couplings with P and CP violation and some internal particles have to go on-shell (Cutkosky cut) to generate the asymmetry.

VI. NUMERICAL RESULTS

First, the polarization asymmetry versus DM mass m_χ for scalar DM with the diphoton final state is shown in Fig. 2. The y -axis is the polarization asymmetry normalized to the total amplitude squared:

$$\frac{|\sum_f \mathcal{M}_f(+, +)|^2 - |\sum_f \mathcal{M}_f(-, -)|^2}{|\sum_f \mathcal{M}_f(+, +)|^2 + |\sum_f \mathcal{M}_f(-, -)|^2} , \quad (59)$$

where we consider b -quark only (top left panel), (b, t) (top right panel) and (τ, c, b, t) (bottom panel) contributions. The blue lines refer to universal couplings $C_f^S = C_f^P$ for all fermions involved, while the purple lines assume the couplings are proportional to the internal fermion mass: $C_f^S = C_f^P \sim m_f/m_\chi$. The vertical red dashed lines indicate the masses of fermions involved.

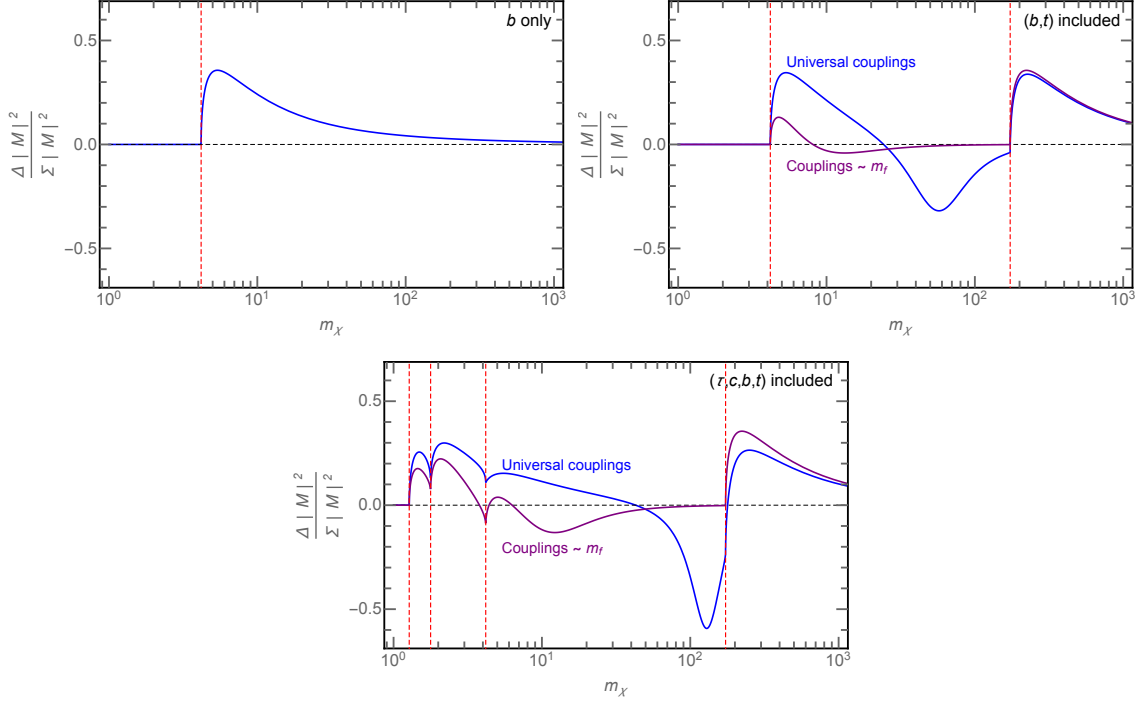


FIG. 2. The polarization asymmetry in the diphoton state for scalar DM with b -quark only (top left), (b, t) (top right) and (τ, c, b, t) (bottom) contributions. The blue lines correspond to universal couplings $C_f^S = C_f^P$ for all fermions involved, while the purple line assumes couplings scale with the fermion mass: $C_f^S = C_f^P \sim m_f/m_\chi$. See text for details.

From the top left panel, it is clear that polarization asymmetry exists when the internal fermion is on-shell for $m_\chi > m_b$. In the top right panel, the blue line exhibits the aforementioned interference effect between heavy-light fermions that can be important for $m_t \geq m_\chi \geq m_b$. In contrast, the purple line does not feature a significant interplay between the quarks because the contributions from b are suppressed by the coupling for $m_\chi \gg m_b$, leading to a small interference. Finally, the bottom panel shows more complicated interference features if more fermions participate in the processes.

Next, we display results for the $Z\gamma$ final state which, unlike the diphoton channel, can actually generate asymmetry in the case of the tensor operator \mathcal{L}_3^D . Note that as the Z boson will eventually decay into SM particles, we sum over all Z polarizations. Therefore, the asymmetry is defined as

$$\frac{|\sum_{f,Z_{\text{pol}}} \mathcal{M}_f(Z_{\text{pol}}, +)|^2 - |\sum_{f,Z_{\text{pol}}} \mathcal{M}_f(Z_{\text{pol}}, -)|^2}{|\sum_{f,Z_{\text{pol}}} \mathcal{M}_f(Z_{\text{pol}}, +)|^2 + |\sum_{f,Z_{\text{pol}}} \mathcal{M}_f(Z_{\text{pol}}, -)|^2}. \quad (60)$$

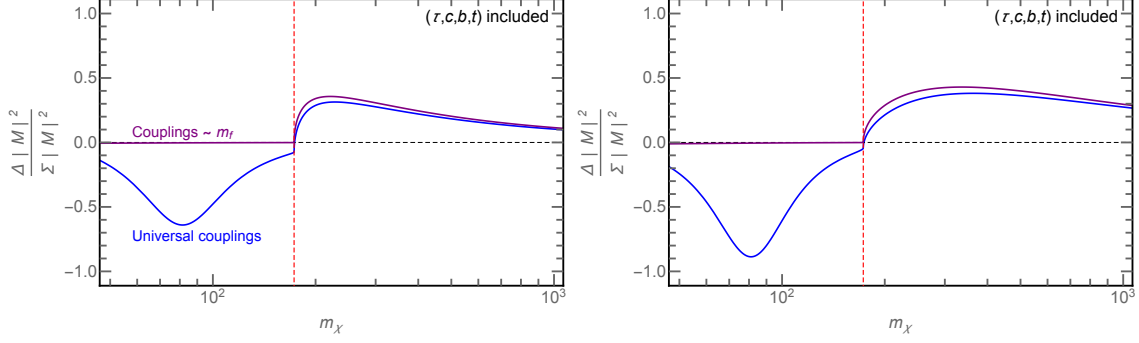


FIG. 3. Similar to Fig. 2 but for the $Z\gamma$ final state. Left: Circular polarization asymmetry for scalar DM with \mathcal{L}^S . Right: Circular polarization asymmetry for fermion DM with the tensor operator \mathcal{L}_3^D .

The left panel of Fig. 3 corresponds to the scalar DM with \mathcal{L}^S , while the right panel presents fermion DM with \mathcal{L}_3^D , both with (τ, c, b, t) included in the loop. As above, we assume a universal coupling $\tilde{C}_{\chi f} = (1+i)/\sqrt{2}$ (blue line) and $\tilde{C}_{\chi f} = \frac{m_f}{m_\chi}(1+i)/\sqrt{2}$ (purple). For simplicity, we confine ourselves to the on-shell Z in the final state such that $m_\chi \geq m_Z/2$. As can be seen from the plots, the interference effect between the heavy-light fermions is more significant in this case. Different operators and coupling choices behave quite similarly with \mathcal{L}_3^D having much larger b -quark contributions and hence stronger interference effects for $m_\chi \gtrsim m_Z/2$ in the presence of the universal coupling.

We conclude this section by showing the ratio of fluxes from the loop-induced $\chi\chi \rightarrow \gamma\gamma$ and continuous γ -ray spectrum from the final state radiation (FSR) of tree-level DM annihilation processes $\chi\chi \rightarrow \bar{f}f\gamma$. The ratio of DM-origin photon numbers in the energy bin of $[m_\chi(1-\epsilon), m_\chi(1+\epsilon)]$ (ϵ : energy resolution of an experiment of interest) between the discrete lines and total contribution reads

$$\frac{N_\gamma^{\text{line}}}{N_\gamma^{\text{total}}} = \frac{2\langle\sigma v\rangle_{\gamma\gamma} 0.68}{2\langle\sigma v\rangle_{\gamma\gamma} 0.68 + \langle\sigma v\rangle_{\bar{f}f}\Delta N_\gamma}, \quad (61)$$

where 0.68 is the probability of the photon line being reconstructed with the energy bin $[m_\chi(1-\epsilon), m_\chi(1+\epsilon)]$, and the prefactor 2 comes from the fact that there are two photons in the final state at each DM annihilation. The symbol ΔN_γ is the number of photons within the energy bin, given a DM annihilation

$$\Delta N_\gamma = \int_{m_\chi(1-\epsilon)}^{m_\chi(1+\epsilon)} \frac{d\Gamma}{dE_\gamma} dE_\gamma, \quad (62)$$

where $\frac{d\Gamma}{dE_\gamma}$ is the FSR photon energy distribution (vanishing if $E_\gamma > m_\chi$) and obtained from PPPC4DMID [20, 21].

In the left panel of Fig. 4, including b and t -quarks only we have shown the ratio of Eq. (61) for universal couplings (blue) with $C_f^S = C_f^P$, and couplings proportional to the mass of fermions (purple) with $C_f^S = C_f^P \sim m_f/m_\chi$, for scalar DM. Note that for $m_\chi \geq m_t$, the annihilation channel $\chi\chi \rightarrow \bar{t}t$ is open. We assume the energy resolution to be 10% (solid lines) and 5% (dashed lines). It is clear that with a better resolution, the discrete component becomes relatively larger as the decreasing bin width reduces the continuous component. Moreover, although $\chi\chi \rightarrow \gamma\gamma$ is loop suppressed, the ratio can still be sizable since the FSR photon spectrum diminishes in limit of $E_\gamma \rightarrow m_\chi$. Finally, for couplings $\sim m_f$ the contributions to photon lines from the t -quark loop is much more important than b -quark, leading to prominent line signals. This scenario mimics the SM Higgs diphoton decay, where the fermion contributions are dominated by the top quark.

In the right panel of Fig. 4, we show a similar plot but replacing the numerator of the ratio (discrete photon number) by the absolute value of the polarized photon number, *i.e.*, $\Delta N_\gamma^{\text{line}} \equiv |N_\gamma(+, +) - N_\gamma(-, -)|$. The asymmetry can be pronounced for $m_\chi \gtrsim m_t$ especially for the case of couplings proportional to masses. It can be understood from the top right panel of Fig. 2 that the asymmetry is sizable when $m_\chi \gtrsim m_t$ and from the fact that the line component dominates for large m_χ as displayed in the left panel of Fig. 4.

The total differential DM-origin photon flux by including all annihilation channels denoted by i from the Galactic Center is

$$\frac{d^2\Phi_\chi^{\text{total}}}{d\Omega dE_\gamma} = \frac{1}{2} \frac{r_\odot}{4\pi} \left(\frac{\rho_\odot}{m_\chi} \right)^2 J \sum_i \langle \sigma v \rangle_i \frac{d\Gamma_i}{dE_\gamma}, \quad (63)$$

where $d\Omega$ is the solid angle, r_\odot is the distance from the Galactic Center to the Sun, ρ_\odot is the local DM density, and J is the J -factor which is the integration of DM contributions along the line of sight. If both DM particle and antiparticle are present, an extra 1/2 is needed. Assume the astrophysical γ -ray background be unpolarized and its differential flux be denoted by

$$\frac{d^2\Phi_{\text{bkg}}}{d\Omega dE_\gamma}. \quad (64)$$

Then, the number of background photons that contributes to the N_γ^{total} in Eq. (61) is given

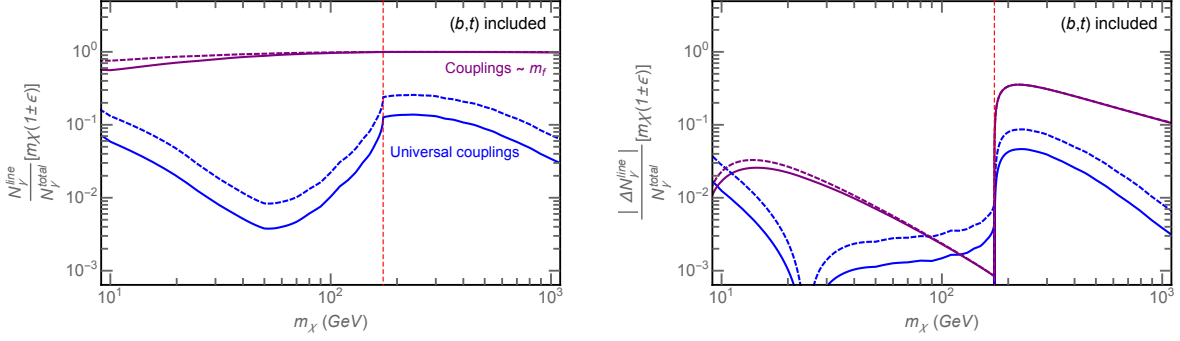


FIG. 4. Left: The number ratio of discrete photons to discrete plus continuous ones. Right: The number ratio of polarized photons to the total DM-origin photons. The blue lines correspond to universal couplings while the purple lines indicate couplings proportional to the mass of fermions in loops. We assume the energy resolution to be 5% (dashed) and 10% (solid). See the text for more details.

by

$$N_\gamma^{\text{bkg}} = \frac{d\Phi_{\text{bkg}}}{d\Omega} \left[\frac{1}{2} \frac{r_\odot}{4\pi} \left(\frac{\rho_\odot}{m_\chi} \right)^2 J \right]^{-1}, \quad (65)$$

where

$$\frac{d\Phi_{\text{bkg}}}{d\Omega} = \int_{m_\chi(1-\epsilon)}^{m_\chi(1+\epsilon)} \frac{d^2\Phi_{\text{bkg}}}{d\Omega dE_\gamma} dE_\gamma.$$

Thus the degree of circular polarization will be lowered by the unpolarized γ -ray background. That can be remedied by increasing the energy resolution of the γ -ray polarimetry to capture the polarized line photons.

VII. PROSPECTS FOR DETECTING A NET CIRCULAR POLARIZATION

The azimuthal angle of the plane of production of an electron-positron pair created in a γ -ray detector provides a way of measuring linear polarization of incoming γ rays. It has been demonstrated that the use of an active target consisting of a time-projection chamber enables the measurement of the linear polarization with an excellent effective polarization asymmetry [22]. The current γ -ray detectors are not designed primarily for polarization measurement. Instruments sensitive to linear polarization will be employed in future γ -ray experiments such as ADEPT, HARPO, ASTROGAM, and AMEGO, with the minimum

detectable polarization (MDP) from a few percents up to 20% [23, 24]. In principle, the measurement of bremsstrahlung asymmetry of secondary electrons produced in Compton scattering off a magnetized or unpolarized target can be used to determine the circular polarization of incoming γ rays. However, no efficient methods using non-Compton scattering techniques for measuring γ -ray circular polarization have been developed to date. Improved or even new techniques for γ -ray circular polarimetry are yet to be explored.

In Ref. [9], the authors have discussed the possibility of detecting the circular polarization asymmetry of the γ -ray flux in future γ -ray polarimetry experiments. Optimistically, to produce one useful event that can be used in the secondary asymmetry measurement would need about 10^3 photons. The total number of useful events required to measure an asymmetry at one sigma level can be estimated by $N_{\text{useful}} \sim (AP_\gamma)^{-2}$, where A is the asymmetry generated by a polarized photon and P_γ is the fraction of circular polarization. In the present work, P_γ can reach 0.4 at $E \sim 200$ GeV. Assuming that $A \sim 0.1$, to detect a 40% polarized DM signal, we must collect a number of γ photons roughly equal to $10^3 N_{\text{useful}} \sim 6 \times 10^5$.

The possible γ -ray excess from the Galactic Center has been suggested by the Fermi-LAT observations [25]. The γ -ray flux at $E \sim 200$ GeV can be fitted by

$$\frac{d^2\Phi_{\text{excess}}}{d\Omega dE_\gamma} \sim 10^{-7} \left(\frac{\text{GeV}}{E_\gamma}\right)^2 \text{GeV}^{-1} \text{cm}^{-2} \text{s}^{-1} \text{sr}^{-1}. \quad (66)$$

Assume the excess γ -ray flux be dominated by the DM signal. Then, the number of γ photons that go through a detector is given by

$$\frac{d^2\Phi_{\text{excess}}}{d\Omega dE_\gamma} 2\epsilon E_\gamma I_{\text{exp}} \Delta\Omega, \quad (67)$$

where I_{exp} is the detector exposure and $\Delta\Omega$ is the subtended solid angle of the Galactic Center. By taking $E = 200$ GeV, $\epsilon = 0.1$, $I_{\text{exp}} = 5000 \text{ cm}^2 \text{ yr}$, and $\Delta\Omega = 0.18$, we find that the number of γ photons is about 3, which is far below the required number. Note that for lighter DM, the increase on the incoming photon flux (Eq. (67)) is unfortunately offset by the decrease of induced polarization asymmetry as shown in the right panel of Fig. 4, leading to the same conclusion. Future γ -ray polarimetry experiments would need to largely improve the asymmetry measurement and the number of useful events. Otherwise, it seems that new technologies for detecting a net circular polarization in photons should be explored.

VIII. CONCLUSIONS

We have studied the possibility for a net circular polarization of the γ rays coming from dark matter annihilations. We have considered the effective couplings between the fermions in the Standard Model and neutral scalar, Dirac, and Majorana dark matter, which annihilate into monochromatic diphoton and Z -photon final states. The circular polarization asymmetry in the diphoton and Z -photon states for the scalar dark matter can be substantial (even up to nearly 90% for the Z -photon channel), provided that P and CP symmetries are violated in the couplings and internal fermions are on-shell. Given the energy resolution of a γ -ray detector at 5 – 10% level, the degree of circular polarization at the dark matter mass threshold can reach 10 – 40% for the dark-matter induced γ -ray flux coming from the Galactic Center. The unknown astrophysical γ -ray background would obscure the detectability. However, we can make use of the line spectrum of the γ -ray flux from dark matter annihilations to single out the polarization signals from the background, if unpolarized, and the continuum photons resulting from annihilating final-state interactions.

ACKNOWLEDGMENTS

We would like to thank Denis Bernard for a private communication. This work was supported in part by the Ministry of Science and Technology (MoST) of Taiwan under grant numbers 107-2119-M-001-030 (KWN) and 107-2119-M-001-033 (TCY). WCH was supported by the Independent Research Fund Denmark, grant number DFF 6108-00623. The CP3-Origins centre is partially funded by the Danish National Research Foundation, grant number DNR90. This work was partially performed at the Aspen Center for Physics, which is supported by National Science Foundation grant PHY-1607611.

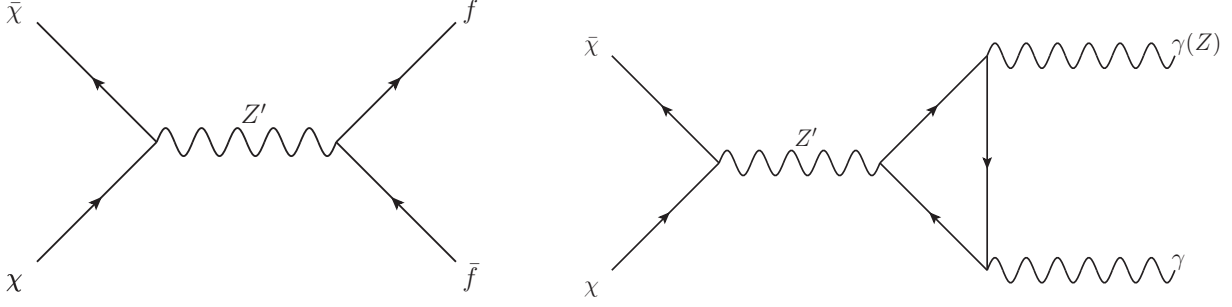


FIG. 5. Left: DM annihilates into SM fermions. Right: DM annihilates into $\gamma\gamma$ or $Z\gamma$ via loop dressing by SM charged fermions.

Appendix A: Z' toy model

We here show that a toy model of an abelian gauge symmetry $U(1)'$ with the corresponding Z' gauge boson will generate the same result as predicted by the effective approach. Assuming both DM particles and SM fermions are charged under the $U(1)'$, thus DM can annihilate into SM fermions via the Z' exchange as shown in the left panel of Fig. 5, as well as the loop-induced $Z\gamma$ and $\gamma\gamma$ channels in the right panel of Fig. 5.

Depending on the $U(1)'$ charge assignment on χ and $f_{L,R}$, the coupling strength can be different for the left-handed and right-handed fields; for instance, in the limit of $m_{Z'} \gg 2m_\chi$, one has for Eq. (3)

$$C_\chi^L = C_\chi^R = C_f^L = C_f^R = 1 \quad \text{and} \quad \frac{(4\pi)^2}{\Lambda^2} = \frac{1}{m_{Z'}^2}. \quad (\text{A1})$$

Note that the loop structure in the UV model is exactly the same as those in the effective approach. As a consequence, one should obtain the same result from the UV model and effective approach. It alludes to the main point in this Appendix that our results only apply to the specific one-loop structure which contains either SM or new fermions only and also the mediator (Z' in this case) has to be heavier than twice the DM mass.

-
- [1] P. A. R. Ade et al. Planck 2015 results. XIII. Cosmological parameters. *Astron. Astrophys.*, 594:A13, 2016, 1502.01589.
- [2] N. Aghanim et al. Planck 2018 results. VI. Cosmological parameters. 2018, 1807.06209.
- [3] M. Tanabashi et al. Review of Particle Physics. *Phys. Rev.*, D98(3):030001, 2018.
- [4] Felix A. Aharonian, Werner Hofmann, and Frank M. Rieger, editors. *Proceedings, 6th International Symposium on High-Energy Gamma-Ray Astronomy (Gamma 2016)*, volume 1792, 2017.
- [5] Alejandro Ibarra, Sergio Lopez-Gehler, Emiliano Molinaro, and Miguel Pato. Gamma-ray triangles: a possible signature of asymmetric dark matter in indirect searches. *Phys. Rev.*, D94(10):103003, 2016, 1604.01899.
- [6] Jason Kumar, Pearl Sandick, Fei Teng, and Takahiro Yamamoto. Gamma-ray Signals from Dark Matter Annihilation Via Charged Mediators. *Phys. Rev.*, D94(1):015022, 2016, 1605.03224.
- [7] W. Bonivento, D. Gorbunov, M. Shaposhnikov, and A. Tokareva. Polarization of photons emitted by decaying dark matter. *Phys. Lett.*, B765:127–131, 2017, 1610.04532.
- [8] Céline Boehm, Céline Degrande, Olivier Mattelaer, and Aaron C. Vincent. Circular polarisation: a new probe of dark matter and neutrinos in the sky. *JCAP*, 1705(05):043, 2017, 1701.02754.
- [9] Andrey Elagin, Jason Kumar, Pearl Sandick, and Fei Teng. Prospects for detecting a net photon circular polarization produced by decaying dark matter. *Phys. Rev.*, D96(9):096008, 2017, 1709.03058.
- [10] Wei-Chih Huang and Kin-Wang Ng. Polarized gamma rays from dark matter annihilations. *Phys. Lett.*, B783:29–35, 2018, 1804.08310.
- [11] Farinaldo S. Queiroz and Carlos E. Yaguna. Gamma-ray lines may reveal the CP nature of the dark matter particle. *JCAP*, 1901:047, 2019, 1810.07068.
- [12] Aneesh Manohar and Howard Georgi. Chiral Quarks and the Nonrelativistic Quark Model. *Nucl. Phys.*, B234:189–212, 1984.
- [13] Kaoru Hagiwara and D. Zeppenfeld. Helicity Amplitudes for Heavy Lepton Production in e^+e^- Annihilation. *Nucl. Phys.*, B274:1–32, 1986.

- [14] R. Mertig, M. Bohm, and Ansgar Denner. FEYN CALC: Computer algebraic calculation of Feynman amplitudes. *Comput. Phys. Commun.*, 64:345–359, 1991.
- [15] Vladyslav Shtabovenko, Rolf Mertig, and Frederik Orellana. New Developments in FeynCalc 9.0. *Comput. Phys. Commun.*, 207:432–444, 2016, 1601.01167.
- [16] T. Hahn and M. Perez-Victoria. Automatized one loop calculations in four-dimensions and D-dimensions. *Comput. Phys. Commun.*, 118:153–165, 1999, hep-ph/9807565.
- [17] G. Passarino and M. J. G. Veltman. One Loop Corrections for $e^+ e^-$ Annihilation Into $\mu^+ \mu^-$ in the Weinberg Model. *Nucl. Phys.*, B160:151–207, 1979.
- [18] Leonard Rosenberg. Electromagnetic interactions of neutrinos. *Phys. Rev.*, 129:2786–2788, 1963.
- [19] Stanley D. Deser, Marc T. Grisaru, and Hugh Pendleton, editors. *Proceedings, 13th Brandeis University Summer Institute in Theoretical Physics, Lectures On Elementary Particles and Quantum Field Theory*, Cambridge, MA, USA, 1970. MIT, MIT.
- [20] Marco Cirelli, Gennaro Corcella, Andi Hektor, Gert Hutsi, Mario Kadastik, Paolo Panci, Martti Raidal, Filippo Sala, and Alessandro Strumia. PPC 4 DM ID: A Poor Particle Physicist Cookbook for Dark Matter Indirect Detection. *JCAP*, 1103:051, 2011, 1012.4515. [Erratum: JCAP1210,E01(2012)].
- [21] Paolo Ciafaloni, Denis Comelli, Antonio Riotto, Filippo Sala, Alessandro Strumia, and Alfredo Urbano. Weak Corrections are Relevant for Dark Matter Indirect Detection. *JCAP*, 1103:019, 2011, 1009.0224.
- [22] P. Gros et al. Performance measurement of HARPO: A time projection chamber as a gamma-ray telescope and polarimeter. *Astropart. Phys.*, 97:10–18, 2018, 1706.06483.
- [23] Jürgen Knödlseder. The future of gamma-ray astronomy. *Comptes Rendus Physique*, 17:663–678, 2016, 1602.02728.
- [24] Alexander Moiseev and On Behalf Of The Amego Team. All-Sky Medium Energy Gamma-ray Observatory (AMEGO). *PoS*, ICRC2017:798, 2018.
- [25] Francesca Calore, Ilias Cholis, and Christoph Weniger. Background Model Systematics for the Fermi GeV Excess. *JCAP*, 1503:038, 2015, 1409.0042.